

This is a repository copy of *NEDA—NEutron Detector Array*.

White Rose Research Online URL for this paper:

<https://eprints.whiterose.ac.uk/id/eprint/144728/>

Version: Accepted Version

---

**Article:**

Valiente-Dobón, J. J., Jaworski, G., Goasduff, A. et al. (56 more authors) (2019) NEDA—NEutron Detector Array. *Nuclear Instruments and Methods in Physics Research, Section A: Accelerators, Spectrometers, Detectors and Associated Equipment*. pp. 81-86. ISSN: 0168-9002

<https://doi.org/10.1016/j.nima.2019.02.021>

---

**Reuse**

This article is distributed under the terms of the Creative Commons Attribution-NonCommercial-NoDerivs (CC BY-NC-ND) licence. This licence only allows you to download this work and share it with others as long as you credit the authors, but you can't change the article in any way or use it commercially. More information and the full terms of the licence here: <https://creativecommons.org/licenses/>

**Takedown**

If you consider content in White Rose Research Online to be in breach of UK law, please notify us by emailing [eprints@whiterose.ac.uk](mailto:eprints@whiterose.ac.uk) including the URL of the record and the reason for the withdrawal request.

# NEDA - NEutron Detector Array

J.J. Valiente-Dobón<sup>a</sup>, G. Jaworski<sup>a</sup>, A. Goasduff<sup>a,b,c</sup>, F.J. Egea<sup>a,b,c,d</sup>,  
V. Modamio<sup>a,e</sup>, T. Hüyük<sup>d</sup>, A. Triossi<sup>b,c,f</sup>, M. Jastrzāb<sup>g</sup>, P.A. Söderström<sup>h</sup>,  
A. Di Nitto<sup>i</sup>, G. de Angelis<sup>a</sup>, G. de France<sup>j</sup>, N. Erduran<sup>k</sup>, A. Gadea<sup>d</sup>,  
M. Moszyński<sup>l</sup>, J. Nyberg<sup>m</sup>, M. Palacz<sup>n</sup>, R. Wadsworth<sup>o</sup>, R. Aliaga<sup>d</sup>,  
C. Aufranc<sup>q</sup>, M. Bézard<sup>j</sup>, G. Baulieu<sup>q</sup>, E. Bissiato<sup>a</sup>, A. Boujrad<sup>j</sup>, I. Burrows<sup>p</sup>,  
S. Carturan<sup>a,b</sup>, P. Cocconi<sup>a</sup>, G. Colucci<sup>b,c</sup>, D. Conventi<sup>a</sup>, M. Cordwell<sup>p</sup>,  
S. Coudert<sup>j</sup>, J.M. Deltoro<sup>a</sup>, L. Ducroux<sup>j</sup>, T. Dupasquier<sup>q</sup>, S. Ertürk<sup>r</sup>,  
X. Fabian<sup>q</sup>, V. González<sup>s</sup>, A. Grant<sup>p</sup>, K. Hadyńska-Kłęk<sup>a,t</sup>, A. Illana<sup>a</sup>,  
M. L. Jurado-Gomez<sup>d</sup>, M. Kogimtzis<sup>p</sup>, I. Lazarus<sup>p</sup>, L. Legeard<sup>j</sup>, J. Ljungvall<sup>u</sup>,  
G. Pasqualato<sup>b,c</sup>, R. M. Pérez-Vidal<sup>d</sup>, A. Raggio<sup>a</sup>, D. Ralet<sup>j</sup>, N. Redon<sup>q</sup>,  
F. Saillant<sup>j</sup>, B. Saygi<sup>v</sup>, E. Sanchis<sup>s</sup>, M. Scarcioffolo<sup>b,c</sup>, M. Siciliano<sup>a</sup>,  
D. Testov<sup>b,c</sup>, O. Stezowski<sup>q</sup>, M. Tripon<sup>j</sup>, I. Zanon<sup>a</sup>

<sup>a</sup>*Istituto Nazionale di Fisica Nucleare, Laboratori Nazionali di Legnaro, Legnaro, Italy*

<sup>b</sup>*Dipartimento di Fisica e Astronomia, Università di Padova, Padova, Italy*

<sup>c</sup>*Istituto Nazionale di Fisica Nucleare, Sezione di Padova, Università di Padova, Padova, Italy*

<sup>d</sup>*Instituto de Física Corpuscular, CSIC-Universidad de Valencia, E-46980 Paterna (Valencia), Spain*

<sup>e</sup>*Department of Physics, University of Oslo, N-0316 Oslo, Norway*

<sup>f</sup>*CERN, Switzerland*

<sup>g</sup>*Niewodniczanski Institute of Nuclear Physics, Polish Academy of Sciences, Kraków, Poland*

<sup>h</sup>*Extreme Light Infrastructure Nuclear Physics (ELI-NP), 077125 Bucharest-Magurele, Romania*

<sup>i</sup>*Helmholtz Institute Mainz and GSI Helmholtzzentrum für Schwerionenforschung Darmstadt, Germany*

<sup>j</sup>*GANIL, CEA/DRF-CNRS/IN2P3, Bvd. Henri Becquerel, 14076 Caen, France*

<sup>k</sup>*Faculty of Engineering and Natural Sciences, Istanbul Sabahattin Zaim University, 34303 Istanbul, Turkey*

<sup>l</sup>*National Centre for Nuclear Research, 05-400 Otwock-Świerk, Poland*

<sup>m</sup>*Department of Physics and Astronomy, Uppsala University, SE-75120 Uppsala, Sweden*

<sup>n</sup>*Heavy Ion Laboratory, University of Warsaw, 02-093 Warsaw, Poland*

<sup>o</sup>*Department of Physics, University of York, Heslington, YO10 5DD York, U.K.*

<sup>p</sup>*STFC Daresbury Laboratory, Daresbury, Warrington WA4 4AD, U.K.*

<sup>q</sup>*Université Lyon 1, CNRS, IN2P3, IPN Lyon, F-69622 Villeurbanne, France*

<sup>r</sup>*Department of Physics, University of Nigde, 51240 Nigde, Turkey*

<sup>s</sup>*Departamento de Ingeniería Electrónica, Universidad de Valencia. Avda. Universidad s/n 46100 Burjassot, Spain.*

<sup>t</sup>*Department of Physics, University of Surrey, Guildford GU2 7XH, U.K.*

<sup>u</sup>*CSNSM, CNRS, IN2P3, Université Paris-Sud, F-91405 Orsay, France*

<sup>v</sup>*Department of Physics, Faculty of Science, University of Ege, Izmir, 35100, Turkey*

---

## Abstract

The NEutron Detector Array, NEDA, will form the next generation neutron detection system that has been designed to be operated in conjunction with  $\gamma$ -ray arrays, such as the tracking-array AGATA, to aid nuclear spectroscopy studies. NEDA has been designed to be a versatile device, with high-detection efficiency, excellent neutron- $\gamma$  discrimination and high rate capabilities. It will be employed in physics campaigns in order to maximise the scientific output, making use of the different European stable and radioactive ion beams. The

50 first implemenation of the neutron detector array NEDA with AGATA  $1\pi$  was  
51 realized at GANIL. This manuscript reviews the various aspects of NEDA.

52 *Keywords:* NEDA, Nuclear structure, gamma-ray spectroscopy, neutron  
53 detector, liquid scintillator, digital electronics, neutron-gamma discrimination

---

## 54 1. Introduction

55 The main objective of nuclear structure is to study the nature and phe-  
56 nomenology of the nucleon-nucleon interaction in the nuclear medium. Gamma-  
57 ray spectroscopy represents one of the most powerful methods to study nuclear  
58 structure since a large fraction of the de-excitation of the excited nuclear levels  
59 goes via the emission of  $\gamma$  rays. High-resolution  $\gamma$ -ray spectroscopy makes it pos-  
60 sible to perform high precision measurements that help to determine the energy,  
61 angular momentum and parity of nuclear excited states, as well as transition  
62 probabilities using a variety of techniques. All this information characterizes  
63 the nucleus under study. The knowledge of nuclear matter has progressed *pari*  
64 *passu* with the technical development of  $\gamma$ -ray spectrometers and associated an-  
65 cillary devices that the nuclear spectroscopy community has built up over the  
66 last five decades.

67 The NEutron Detector Array (NEDA) [1, 2, 3, 4, 5, 6, 7, 8] is a neutron  
68 detector array of the next generation. It has been constructed as an ancillary  
69 detector for use with the Advanced Gamma Tracking Array (AGATA), which is  
70 a state-of-the-art high-resolution  $\gamma$ -ray spectrometer based on the  $\gamma$ -ray tracking  
71 technique [9]. The first implementation of NEDA has been done with AGATA  
72  $1\pi$  at GANIL [1, 10]. However, other large  $\gamma$ -ray arrays are also foreseen to  
73 be coupled to NEDA. Neutron and charged-particle detectors provide a good  
74 selection of the decay channels that has been demonstrated to be very efficient  
75 for the study of neutron-deficient nuclei populated by fusion-evaporation re-  
76 actions, e.g. for the investigation of nuclei close to the  $N=Z$  line. NEDA is  
77 also a well suited device for the investigation of exotic nuclei populated with  
78 transfer reactions, where the emitted particle is a neutron. A large variety of  
79 new radioactive beams will be accessible in the next years for transfer reactions  
80 induced by proton- and neutron-rich projectiles from radioactive beam facilities  
81 such as HIE-ISOLDE (CERN, Geneva, Switzerland), SPES (Legnaro, Italy),  
82 SPIRAL2 (Caen, France) and FAIR (Darmstadt, Germany). Neutron detectors  
83 based on liquid scintillators that provide neutron- $\gamma$  identification by pulse-shape  
84 discrimination and Time-of-Flight (ToF) have been in use for decades. There  
85 are a few examples of high-efficiency neutron detectors with high discrimination  
86 capabilities between neutrons and  $\gamma$  rays that can be coupled to large  $\gamma$ -ray  
87 arrays, such as Neutron Wall [11, 12], Neutron Shell [13] and DESCANT [14].

88 The conceptual design of NEDA is discussed in Section 2. The outcome of  
89 our considerations for a broad use of NEDA in different experimental conditions  
90 yielded a design based on a modular array of hexagonal single detectors that can  
91 tile up a compact surface or a hemisphere, see Section 3. Section 4 describes  
92 the fully-digital front-end electronics conceived to obtain excellent neutron- $\gamma$   
93 discrimination capabilities, integration with fully digital modern  $\gamma$ -ray arrays  
94 and flexibility. Finally, Section 5 discusses the data-acquisition system imple-  
95 mented for NEDA and AGATA.

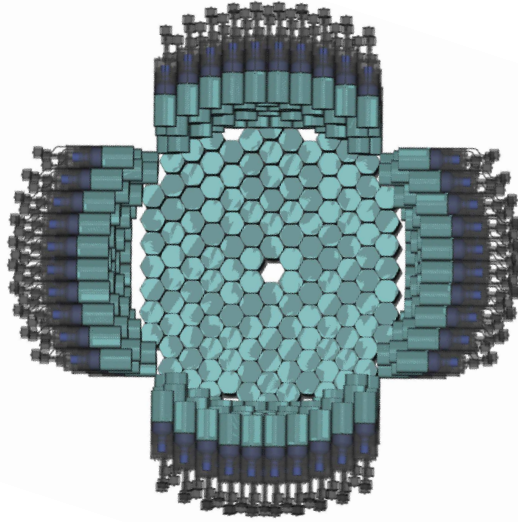


Figure 1: Proposed NEDA geometry for a  $2\pi$  angular coverage at one meter distance. The total number of identical NEDA detectors is 331, covering a solid angle of  $1.88 \pi$  s.r.

## 2. Conceptual design

NEDA is conceptually designed to be a versatile and a highly-efficient neutron detector array with good neutron- $\gamma$  discrimination capabilities at high counting rates. It will be used as a neutron tagging instrument coupled with large  $\gamma$ -ray arrays at stable and radioactive ion beam facilities, that will efficiently measure neutrons emitted from outgoing channels in fusion-evaporation and low-energy transfer reactions. The kinematics of particles emitted in these two types of nuclear reactions, fusion-evaporation and transfer, demand very different characteristics from a neutron detector. In the former case, the neutrons have a Maxwellian distribution with a maximum at energies of a few MeV and due to the kinematics of the reaction, they have an angular distribution peaked at forward angles with respect to the beam direction. NEDA has specially been optimised to have large efficiency in such fusion-evaporation reactions, for neutron multiplicities 2 and 3. In transfer reactions, the neutrons can reach energies above 10 MeV and their angular distributions highly depend on the angular momentum transferred, energy of the beam, and kinematics of the reaction.

An early implementation of NEDA combined with Neutron Wall and AGATA for fusion-evaporation reactions is described in Ref. [1]. In this first usage of NEDA, a limited number of NEDA detectors were coupled together with the Neutron Wall at approximately half a meter from the target with an angular

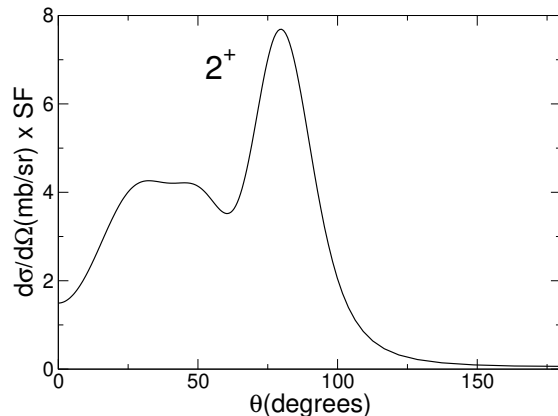


Figure 2: Calculated cross sections for the  $2^+$  state with Twofnr [15] as a function of the angle of the emitted neutrons in the laboratory reference frame for the reaction  ${}^3\text{He}({}^{18}\text{Ne},n){}^{20}\text{Mg}$  at 4.0 MeV $\times$ A. SF is the spectroscopic factor, that has been considered one for this case.

coverage of  $1.6 \pi$  s.r. In this reference, a large discussion was dedicated to the validation of the GEANT4 simulations with experimental data. Whereas, the present work is devoted to a discussion of the NEDA  $2\pi$  configuration, which will be composed of 331 single NEDA detectors located one meter from the target and covering a solid angle of  $1.88 \pi$  s.r.. The angular coverage for each individual detector is about  $7.5^\circ$ . This configuration will allow for an improvement of not only neutron- $\gamma$  discrimination, based on Time-Of-Flight (TOF) measurements but also the neutron angular resolution, which is essential for measuring, in transfer reactions, the angular momentum transferred. The geometry for the NEDA  $2\pi$  configuration at one meter focal distance is shown in Fig. 1. Simulations for this geometry were performed by using the previously developed event generator for GEANT4 simulations, producing neutrons emitted by a  ${}^{252}\text{Cf}$  source and in the fusion-evaporation reaction  ${}^{58}\text{Ni} + {}^{56}\text{Fe}$  at 220 MeV [1]. In addition, a possible future transfer reaction to be used with NEDA has been considered in the simulations, namely  ${}^3\text{He}({}^{18}\text{Ne},n){}^{20}\text{Mg}$  at 4.0 MeV $\times$ A. For this latter case an isotropic angular distribution as well as a realistic angular distribution for the neutrons, calculated with the DWBA Twofnr code [15], has been used as the event-generator input for the GEANT4 simulations. The flat angular distribution is purely an academic exercise, where the important parameter that will affect the efficiencies is the neutron energy. Figure 2 shows the calculated cross sections for the  $2^+$  state as a function of the angle of the emitted neutron in the laboratory reference frame.

Table 1 shows the simulated one-, two- and three-neutron detection efficiencies for emissions from a  ${}^{252}\text{Cf}$  (*Cf*) source and from the fusion-evaporation reaction  ${}^{58}\text{Ni} + {}^{56}\text{Fe}$  at 220 MeV (*FE*) for a light threshold of 50 keVee. The one-neutron efficiency obtained for the transfer reaction  ${}^3\text{He}({}^{18}\text{Ne},n){}^{20}\text{Mg}$  at 4.0 MeV per nucleon is also shown. A full angular dependence (*TA*) and a flat distribution (*TF*) have been considered for this physics case. For this study cases (*TA* and *TF*), the neutrons have an energy of 17 MeV at zero degrees and around 3 MeV at ninety degrees. The simulation that considers the real angular distribution will reflect, in addition to the efficiency for the large energy neutrons, the angular integrated cross-section which is very much dependent

Table 1: One-, two- and three-neutron detection efficiencies obtained from simulations of a  $^{252}\text{Cf}$  source (*Cf*) and the fusion-evaporation reaction,  $^{58}\text{Ni}$  (220 MeV) +  $^{56}\text{Fe}$  (*FE*). The one-neutron efficiency, simulated for the transfer reaction  $^3\text{He}(^{18}\text{Ne},n)^{20}\text{Mg}$  at 4.0 MeV per nucleon, is also shown. For this case a full angular dependence (*TA*) and an isotropic distribution of the emitted neutron (*TF*) have been considered. The final values of the efficiencies have been scaled by the correction factor discussed in Ref. [1]. Results obtained for a light threshold of 50 keVee. Errors quoted are statistical.

Geometry	$\varepsilon_{1n}$ [%]	$\varepsilon_{2n}$ [%]	$\varepsilon_{3n}$ [%]
NEDA $2\pi$ - Cf	23.82(15)	4.33(7)	0.63(3)
NEDA $2\pi$ - FE	40.54(7)	11.49(9)	3.7(2)
NEDA $2\pi$ - TA	42.75(7)	-	-
NEDA $2\pi$ - TF	18.67(4)	-	-

on each specific beam and target combination, the angular momentum transferred and the energy of the beam. The simulations of the NEDA  $2\pi$  version at one meter focal distance can not be directly compared to the results presented in Ref. [1] since in the present simulation a 50 keVee threshold has been utilised, whereas the simulations presented in Ref. [1] were performed with a threshold of 150 keVee for the NEDA detectors and an individual threshold for each Neutron Wall detector. For transfer reactions were high energy neutrons are involved the full NEDA array still keeps a large efficiency as can be seen in Table 1 for the case of a isotropic angular distribution. This is because the NEDA detectors have a significant intrinsic neutron detection efficiency due to their depth of around 20 cm. In addition to the large efficiency of the NEDA  $2\pi$  at one meter focal distance, one should consider other aspects: among those aspects it is worth noticing that by exploiting the larger flight path it will be possible to improve the neutron- $\gamma$  discrimination and the energy resolution, due to the longer TOF, as well as the angular resolution, due to the smaller solid angles subtended by each single detector.

### 3. Detectors

The single NEDA detector was carefully designed in order to achieve the best possible efficiency, time resolution, neutron- $\gamma$  discrimination and minimise cross-talk among detectors. Extensive Monte Carlo simulations were carried out to optimise the type of scintillator used, the size of a single detector and its distance to the target and thus the granularity of the array [2]. The final decision was to build individual NEDA detectors with a cross-section fitting a 5 inch Photo Multiplier Tube (PMT) with a length of around 20 cm. The active volume of the detector was filled with the liquid scintillator ELJEN EJ301 (which is equivalent to BC501A). Furthermore, since a highly efficient array was foreseen, a fully tiled up surface was required, with minimum dead layers in between. Only three regular polygons (square, triangle, hexagon) can tile a flat surface without gaps. This can be done by using only one type of these polygons or a combination of several of them. One of the polygons, the regular hexagon, was chosen as the starting point for the NEDA geometry since its profile covers the largest fraction of the area of a photomultiplier with a circular cross section.

A single NEDA detector is shown in Fig. 3. The detector cell is made of 6060 aluminium alloy and has a hexagonal profile with a 146 mm side to side distance, and 3 mm thick walls. It is 205 mm long, with an active volume of

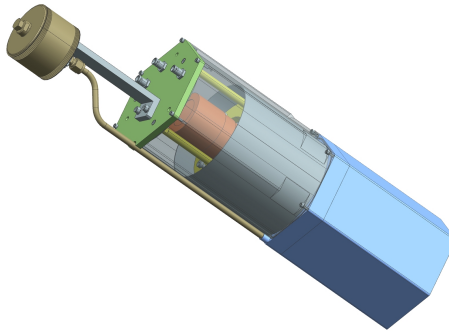


Figure 3: Drawing showing the design of a NEDA neutron detector. It has a hexagonal profile with a cell (blue) where the liquid organic scintillator EJ301 is placed. This cell is connected via a pipe to an expansion bellow (brown). A hexagonal light tight casing contains the Photo Multiplier Tube and voltage divider (orange) as well as a mu-metal shielding (grey). The spring pusher for the PMT is shown in yellow.

~3.15 litres filled with the liquid organic scintillator EJ301. The inner surface is coated with TiO<sub>2</sub>-based reflective paint EJ520. The top flange includes a 5 inch N-BK7 5 mm thick glass window, which has 92% transmittance for the wavelength spectrum emitted by the scintillator. A pipe connects the active volume of the detector with an expansion chamber located on the top of the PMT casing. This expansion chamber is needed to allow for the change in volume of the scintillator with temperature. The edge welded bellow (expansion chamber) is 3 inch in diameter and expands up to 153 cm<sup>3</sup> in a stroke of 4.8 cm, leading to an operational temperature range of 40 °C with minimal pressure differences. The design of a single NEDA detector has been already described in Ref. [16].

An investigation into the best possible PMT existing in the market that would provide good neutron- $\gamma$  discrimination, as well as the best possible timing, was performed and published in Ref. [3]. From the various PMTs on the market (ET9390-kb produced by ET Enterprises and the Hamamatsu R4144 and R11833-100), it was shown that ET9390-kb and R11833-100 are of similar quality giving a Figure Of Merit (FOM), as defined in Ref. [17] of  $\approx 1.7$  at  $320 \pm 20$  keVee for a commercial test detector, which was significantly better than R4144. Taking into account also the timing properties of the three PMTs, thoroughly discussed in Ref. [4], the final choice was the Hamamatsu PMT of model R11833-100 with a super bi-alkali photocathode. The voltage divider, designed and constructed within the collaboration for the R11833-100 PMT, is transistorised in order to sustain large counting rates without losing linearity. Successful linearity tests were performed up to counting rates of  $\sim 300$  kHz.

The final detector, which is self produced by the NEDA collaboration, has an excellent light yield of  $2850 \pm 100$  photoelectrons per MeVee. The average value is almost a factor of two larger than what was obtained for the previously developed detectors for the EUROBALL Neutron Wall [11]. Figure 4 shows a typical neutron- $\gamma$  discrimination, based on the charge comparison method [17], as a function of light yield in keVee measured with a <sup>252</sup>Cf source. One can note, the excellent separation of the  $\gamma$  and neutron distributions even for such large scintillator volume.

Further detailed information on the design, construction, tests and performance of a single NEDA detector will be provided in a forthcoming publication [18].

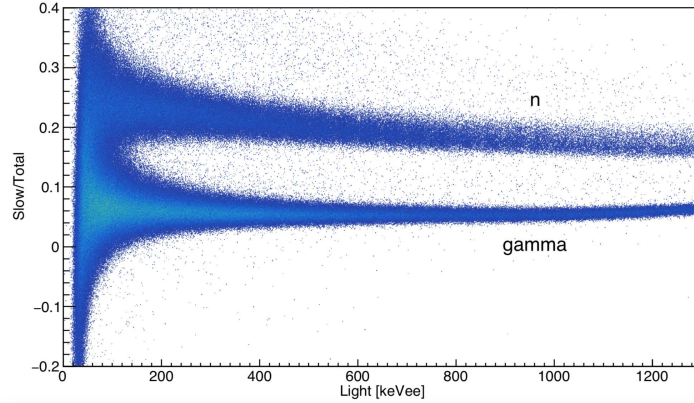


Figure 4: Pulse-shape discrimination based on the charge comparison method [17] measured with a NEDA detector using a  $^{252}\text{Cf}$  source. The ratio of the light in the slow component of the digitised signal divided by the total light is shown on the y axis as a function of the total light in keVee on the x axis.

#### 4. Front-end electronics

NEDA Front-End Electronics (FEE), unlike its predecessor the Neutron Wall, is fully-digital and envisaged to improve the neutron- $\gamma$  discrimination, as well as the processing capabilities, integration and overall flexibility [5]. As mentioned before, NEDA is primarily designed to be used together with various Ge detector systems, in particular with AGATA, EXOGAM2 [19, 20] and the GALILEO [21] arrays. In order to facilitate this coupling, the electronics of NEDA uses the Global Trigger and Synchronisation (GTS) system [22].

The detector photomultiplier tube delivers a current signal through a 15-m-long shielded coaxial cable to a NIM module that provides the Single-Ended to DIFFerential (SE-DIFF) conversion. SE-DIFF delivers differential analog signals to the digitizers and pre-processing modules by means of HDMI cables. These two sets of cables have been selected carefully to cope with the signal bandwidth and crosstalk performance requirements of NEDA. The shielded coaxial 15-m cables have a -0.43 dB @ 480 MHz. While the 1.5-m HDMI cables have a bandwidth of 430 MHz and crosstalk levels of -42.29/-48.11 dB for signals with rise-times of 3 and 7 ns, respectively.

The SE-DIFF module has been developed in the NIM standard and contains a PCB board capable of converting the signals of 16 detectors. The board uses a fully-differential amplifier AD8139 and each channel is adapted to work in a range of 3 V, although the input range can be increased up to 8 V, activating a voltage divider available at the input stage.

The core of the FEE is the NUMEXO-2 cards developed for EXOGAM2, which consist of a set of 4 Flash Analog-to-Digital-Converter (FADC) Mezzanines in charge of digitising the signals at 200 Msps. The FADC mezzanines



contain each four Analog-to-Digital (A/D) modules. In addition, the cards contain a motherboard which includes two large FPGAs used to perform the trigger generation, digital signal processing, clocking, data packaging and readout tasks to the servers for 16 independent channels.

The FADC Mezzanine is the daughterboard in charge of the A/D conversion, whose sampling frequency and resolution specifications have been selected on the basis of the signal properties to be digitised [6, 7]. These specifications do not come only from the NEDA project since the FADC Mezzanines were also designed for other projects such as EXOGAM2. The major resolution constraint comes from the EXOGAM side whose specification of 2.3 keV @ 1.33 MeV led to a choice of an ADC with ENOB > 11.3. To fulfil the various needs of NEDA and EXOGAM2 the final choice was to use the ADS62P49 sampling device, providing a board with 4 channels sampling at 200 Mps with an ENOB of 11.6-11.7 bits. As for the clock, the main 100 MHz clock from the GTS is obtained, and processed with a jitter cleaner in order to produce a 200 MHz sampling clock. At the input of the FADC Mezzanine, an analog fully-differential coupling stage adapts the input range to the ADC chip range, with the added capability of a controllable offset which permits use of the full FADC dynamics.

The NUMEXO-2 motherboard includes two FPGAs, a Virtex-6 and a Virtex-5, which carry out the pre-processing tasks. The Virtex-6 FPGA performs the data processing, trigger elaboration, package building and formatting, whereas the Virtex-5 FPGA manages the readout via PCIe, slow control via Ethernet, integration of the GTS leaf and implementation of the ADC interface, which is the block in charge of storing temporarily the data before validation by the GTS system. A descriptive view of how the blocks are structured inside the FPGA is depicted in Fig. 5. In the following paragraphs the functionalities included in the two NUMEXO-2 FPGAs will be discussed.

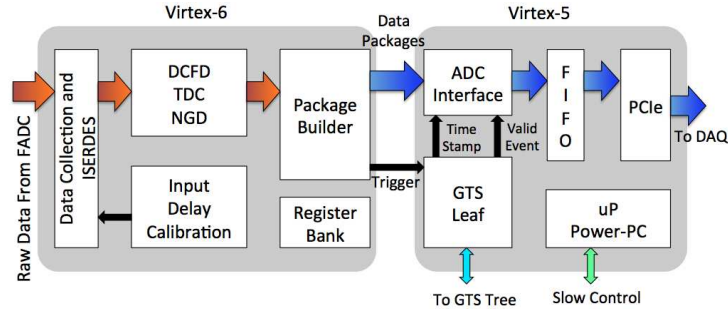


Figure 5: Block diagram depicting the main blocks in the NUMEXO-2 as well as the interaction among them.

The first block found at the beginning of the Virtex-6 is a customized arrangement of serialization/deserialization sub-blocks (called ISERDES), used to convert the multiplexed bit pairs provided from the FADCs into processable samples. After that, the first component that the data finds is a baseline cancellation block and a first-level local trigger based either on a leading edge or a Digital Constant Fraction Discriminator (DCFD). The first-level trigger enables a Pulse Shape Analysis (PSA) for neutron- $\gamma$  discrimination based on

279 the charge-comparison method [17], that will provide the Trigger Request used  
 280 in the GTS Validation/Rejection cycle [22]. Note that, for this block, param-  
 281 eters such as the fast and slow signal component integration times, as well as  
 282 the discrimination threshold, are programmable. In parallel, a Time-of-Flight  
 283 evaluation is done with a TDC process in the FPGA, calculating the time be-  
 284 tween the DCFD zero-crossover signal and an external reference signal, which  
 285 is normally provided by the accelerator. The Trigger Request could be also  
 286 generated by a time condition on the TDC result and can be combined with  
 287 the PSA Trigger Request with boolean AND or OR conditions. Eight LVDS  
 288 data lanes communicating with both FPGAs at rates up to 400 MB/s allow  
 289 a sustained counting rate of 20 kHz trigger request in the 16 channels present  
 290 in the NUMEXO-2 board. The data frames created in the Virtex-6 FPGA are  
 291 compatible with the MFM GANIL data format specification. As mentioned  
 292 in the previous sub-section, the GTS standard has been chosen for NEDA. A  
 293 specific implementation of the GTS leaf, supporting the 16 Trigger Request of a  
 294 NEDA NUMEXO-2 board, has been implemented in the Virtex-5 FPGA. The  
 295 ADC interface process stores temporarily the data buffers and waits for the GTS  
 296 validation prior to sending the evaluated and sample data information via the  
 297 PCIe interface. NEDA uses the NUMEXO-2 4x PCIe v1.0 Endpoint link to read  
 298 out the data. The data are sent to a server (one server per NUMEXO-2) via  
 299 an MPO optical fibre. On the receiver side, a commercial PCIe bridge card is  
 300 hosted in the server and converts the optical input to the PCIe legacy bus stan-  
 301 dard. The Virtex-5 FPGA includes a PowerPC (PPC) 440 processor, running  
 302 an embedded Linux OS, that manages the slow control and GTS services.

## 303 5. Data acquisition

304 In its first implementation at GANIL, the array was used together with  
 305 AGATA, DIAMANT [23] and the Neutron Wall. In this setup, a total of 54  
 306 NEDA detectors and 42 Neutron Wall detectors were used. The signals from  
 307 the 96 neutron detectors were digitised by six NUMEXO-2 cards. In order to  
 308 ensure compatibility of the data acquisition systems of NEDA and AGATA, the  
 309 choice was made to base the data acquisition on the NARVAL system. This sys-  
 310 tem, developed by IPN Orsay, uses the ADA language to manage the data flux  
 311 through several steps from the producer receiving the data from the electronics  
 312 down to the event reconstruction and merging of NEDA data together with the  
 313 AGATA and DIAMANT data. The architecture of the acquisition system for  
 314 one NUMEXO-2 board is presented in Fig. 6. The transmission of the data  
 315 between the different actors is integrated in the NARVAL system and based on  
 316 the TCP/IP and InfiniBand protocols for actors located on separated servers,  
 317 or UNIX FIFO for actors on the same server. Thanks to the flexibility of the  
 318 NARVAL system C++ actors developed, within the AGATA-NEDA collabora-  
 319 tion, are in charge of the data treatment and can be integrated through shared  
 320 libraries loaded in the NARVAL environment.

321 In Section 4, it was shown that the slow-control and the alignment of the  
 322 GTS system is controlled through the ethernet. To ensure the time alignment  
 323 of the GTS of NEDA and AGATA, the NUMEXO-2 boards are inserted in a  
 324 sub-network of the AGATA electronics network. The data transfer of the raw  
 325 events corresponding to a header containing the channel identification and tim-  
 326 ing information is made through a dedicated optical link. Thus, each of the 6

327 NUMEXO-2 boards necessary to accommodate the 96 channels of the NEDA-  
 328 NeutronWall array, plus one spare board, are optically connected to dedicated  
 329 servers in charge of the data pre-processing. Commercial PCI-express optical  
 330 bridges from Samtec are used to make the link between the NUMEXO-2 digitiz-  
 331 ers and the servers. After this optical transmission, the processed data transit  
 332 through two different networks: the GANIL network, where all the local pro-  
 333 cessing of the data and the storage of the raw events is done and the AGATA  
 334 network, on which the two data (NEDA and AGATA) sets are combined. A  
 335 schematic view of the data acquisition system is shown in Fig. 6.

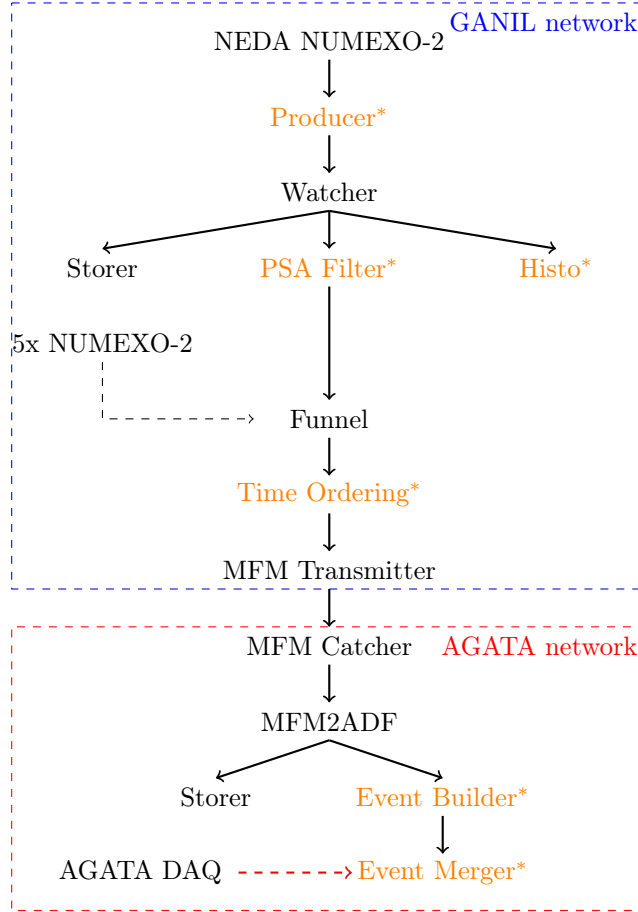


Figure 6: Schematic view of the NEDA data acquisition system. The actors marked with an asterisk are actors developed in C++ within the collaboration. The other actors are standard NARVAL actors. The NEDA acquisition system is shared between two networks: the GANIL and the AGATA network. The transmission of the data between the two networks is performed by one bridge.

336 A dedicated C++ actor, called Producer in Fig. 6, has been developed to  
 337 extract the events from the Direct Memory Access (DMA) and transmit them  
 338 into the NARVAL environment. The data are then transmitted to a standard  
 339 actor which is in charge of copying the data to three different branches and  
 340 sending them to three actors: i) a storer, which is used to remotely store the

full events with the captured traces (digitised signals) on disk that allows for reprocessing the events offline with advanced PSA algorithms such as a Neural Network (NN) [24, 25], ii) a histogrammer, indicated by Histo in Fig. 6, for data quality monitoring, and, finally, iii) an online PSA code.

Three different algorithms have been implemented in the PSA Filter: a Charge-Comparison (CC) algorithm, similar to the one used at the FPGA level, an integrated rise-time algorithm and finally the Neural Network algorithm described in Ref. [25]. In order to limit the quantity of data transmitted on the network, the choice was made to discard the traces at the output of the PSA filter. The reduced frame, containing only the parameters out of the pulse shape algorithms and the frame header are transmitted through Ethernet to a server, where a NARVAL actor concatenates the data from the 6 servers into a single output transmitted to a time ordering filter. This stage of time ordering is essential as the Funnel in Fig. 6 only loops over the 6 inputs and passes the input buffers in the order of the input branches. It is also for this reason, that the detectors are distributed over the different boards in a pie like configuration in order to distribute the counting rate on each of them as equally as possible. It is only after the time sorting that the data are transmitted frame-by-frame to the AGATA acquisition system, in a manner similar to that used for the VAMOS++ campaign [10], namely by using the MFMTxmitter and MFMCatcher actors. Once in the AGATA world, the MFM frames are encapsulated into AGATA Data Format (ADF) frames using a dedicated key. In order to make the replay of the data faster, a storer is implemented at the output of this actor. Indeed, this allows offline building of the NEDA events directly in the AGATA world without having to do a full PSA analysis of the traces. Before merging the NEDA and AGATA data together, the NEDA events are reconstructed in order to extract the real neutron multiplicity using neutron scattering algorithms.

## 6. Summary

The NEutron Detector Array, NEDA, has been designed to be a versatile device, with high detection efficiency, excellent neutron- $\gamma$  discrimination and high count rate capabilities. NEDA will be used together with large  $\gamma$ -ray arrays at stable and radioactive beam facilities such as HIE-ISOLDE (CERN, Geneva, Switzerland), LNL/SPES (Legnaro, Italy), GANIL/SPIRAL2 (Caen, France) and FAIR (Darmstadt, Germany). The physics challenges that NEDA will be facing in the near future will be the study of neutron-deficient nuclei populated with fusion-evaporation reactions, close to  $N=Z$  as well as transfer studies where the emitted particles are neutrons. NEDA will be comprised of 331 detectors, filled with EJ301 liquid scintillator, where each single detector has an hexagonal profile that allows for a fully tiled up surface. The detector cross-section fits a 5 inch Photo Multiplier Tube (PMT) and it has a length of around 20 cm. A photomultiplier with a super bialkali photocathode (R11833-100) and a transistorised voltage divider to sustain large counting rates are used for the read out. The detectors, which are self-made by the NEDA collaboration, have excellent neutron- $\gamma$  discrimination and timing properties. The NEDA front-end electronics is fully digital and uses the Global Trigger and Synchronisation system to improve processing capabilities, flexibility and integration with other detector systems, in particular  $\gamma$ -ray arrays such as AGATA. The core of the front-end electronics are the NUMEXO-2 cards that consist of a set of four

389 FADC Mezzanines, each containing four 200 Msps digitisers. The motherboards  
 390 of the cards contain two FPGA units, a Virtex-6 and a Virtex-5, which carry  
 391 out the pre-processing tasks. The data acquisition system of NEDA in its first  
 392 implementation with AGATA is based on the NARVAL system.

## 393 7. Acknowledgements

394 This study is supported by the Swedish Research Council (contract number  
 395 VR 2014-6644), the Scientific and Technological Research Council of Turkey  
 396 (TUBITAK Project No: 117F114), the Polish National Science Centre, grants  
 397 nos. 2017/25/B/ST2/01569 and 2016/22/M/ST2/00269 COPIN-IN2P3 and  
 398 COPIGAL projects, the UK STFC under grant nos. (ST/J000124/1, ST/L005727/1,  
 399 STL005735/1, ST/P003885/1), the Generalitat Valenciana and MICIU, Spain,  
 400 grants PROMETEO II/2014/019, FPA2017-84756-C4, Severo Ochoa SEV-2014-  
 401 0398 and and by the E.C. FEDER funds.

## 402 References

- 403 [1] T. Hüyük, A. Di Nitto, G. Jaworski, A. Gadea, J. J. Valiente-Dobón, J. Ny-  
 404 berg, M. Palacz, P.-A. Söderström, R. J. Aliaga-Varea, G. de Angelis, et al.,  
 405 Conceptual design of the early implementation of the neutron detector ar-  
 406 ray (neda) with agata, *The European Physical Journal A* 52 (3) (2016)  
 407 1–8.
- 408 [2] G. Jaworski, M. Palacz, J. Nyberg, G. De Angelis, G. De France,  
 409 A. Di Nitto, J. Egea, M. Erduran, S. Ertürk, E. Farnea, et al., Monte carlo  
 410 simulation of a single detector unit for the neutron detector array neda,  
 411 *Nuclear Instruments and Methods in Physics Research Section A: Accel-  
 412 erators, Spectrometers, Detectors and Associated Equipment* 673 (2012)  
 413 64–72.
- 414 [3] X. Luo, V. Modamio, J. Nyberg, J. Valiente-Dobón, Q. Nishada, G. De An-  
 415 gelis, J. Agramunt, F. Egea, M. Erduran, S. Ertürk, et al., Test of digital  
 416 neutron–gamma discrimination with four different photomultiplier tubes  
 417 for the neutron detector array (neda), *Nuclear Instruments and Methods  
 418 in Physics Research Section A: Accelerators, Spectrometers, Detectors and  
 419 Associated Equipment* 767 (2014) 83–91.
- 420 [4] V. Modamio, J. Valiente-Dobón, G. Jaworski, T. Hüyük, A. Triossi,  
 421 J. Egea, A. Di Nitto, P.-A. Söderström, J. A. Ros, G. De Angelis, et al.,  
 422 Digital pulse-timing technique for the neutron detector array neda, *Nu-  
 423 clear Instruments and Methods in Physics Research Section A: Accelera-  
 424 tors, Spectrometers, Detectors and Associated Equipment* 775 (2015) 71–  
 425 76.
- 426 [5] F. E. Canet, V. González, M. Tripon, M. Jastrzab, A. Triossi, A. Gadea,  
 427 G. De France, J. Valiente-Dobón, D. Barrientos, E. Sanchis, et al., Digital  
 428 front-end electronics for the neutron detector neda, *IEEE Transactions on  
 429 Nuclear Science* 62 (3) (2015) 1063–1069.

- [6] F. E. Canet, V. González, M. Tripon, M. Jastrzab, A. Triossi, A. Gadea, G. De France, J. Valiente-Dobón, D. Barrientos, E. Sanchis, et al., A new front-end high-resolution sampling board for the new-generation electronics of exogam2 and neda detectors, *IEEE Transactions on Nuclear Science* 62 (3) (2015) 1056–1062.
- [7] F. J. Egea, E. Sanchis, V. González, A. Gadea, J. M. Blasco, D. Barrientos, J. V. Dobón, M. Tripon, A. Boujrad, C. Houarner, et al., Design and test of a high-speed flash adc mezzanine card for high-resolution and timing performance in nuclear structure experiments, *IEEE Transactions on Nuclear Science* 60 (5) (2013) 3526–3531.
- [8] X. L. Luo, V. Modamio, J. Nyberg, J. J. Valiente-Dobon, Q. Nishada, G. De Angelis, J. Agramunt, F. J. Egea, M. N. Erduran, S. Erturk, G. De France, A. Gadea, V. González, A. Goasduff, T. Hüyük, G. Jaworski, M. Moszyński, A. Di Nitto, M. Palacz, P.-A. Söderström, E. Sanchis, A. Triossi, R. Wadsworth, Pulse pile-up identification and reconstruction for liquid scintillator based neutron detectors, *Nuclear Inst. and Methods in Physics Research*, A 897 (2018) 59–65.
- [9] S. Akkoyun, A. Algora, B. Alikhani, F. Ameil, G. De Angelis, L. Arnold, A. Astier, A. Atac, Y. Aubert, C. Aufranc, et al., Agata: advanced gamma tracking array, *Nuclear Instruments and Methods in Physics Research Section A: Accelerators, Spectrometers, Detectors and Associated Equipment* 668 (2012) 26–58.
- [10] E. Clément, C. Michelagnoli, G. de France, H. Li, A. Lemasson, C. B. Dejean, M. Beuzard, P. Bougault, J. Cacitti, J.-L. Foucher, et al., Conceptual design of the agata  $1\pi$  array at ganil, *Nuclear Instruments and Methods in Physics Research Section A: Accelerators, Spectrometers, Detectors and Associated Equipment* 855 (2017) 1–12.
- [11] Ö. Skeppstedt, H. Roth, L. Lindström, R. Wadsworth, I. Hibbert, N. Kellsall, D. Jenkins, H. Grawe, M. Górski, M. Moszyński, et al., The euroball neutron wall—design and performance tests of neutron detectors, *Nuclear Instruments and Methods in Physics Research Section A: Accelerators, Spectrometers, Detectors and Associated Equipment* 421 (3) (1999) 531–541.
- [12] J. Ljungvall, M. Palacz, J. Nyberg, Monte carlo simulations of the neutron wall detector system, *Nuclear Instruments and Methods in Physics Research Section A: Accelerators, Spectrometers, Detectors and Associated Equipment* 528 (3) (2004) 741–762.
- [13] D. Sarantites, W. Reviol, C. Chiara, R. Charity, L. Sobotka, M. Devlin, M. Furlotti, O. Pechenaya, J. Elson, P. Hausladen, et al., Neutron shell: a high efficiency array of neutron detectors for  $\gamma$ -ray spectroscopic studies with gammasphere, *Nuclear Instruments and Methods in Physics Research Section A: Accelerators, Spectrometers, Detectors and Associated Equipment* 530 (3) (2004) 473–492.
- [14] P. E. Garrett, DESCANT – the deuterated scintillator array for neutron tagging, *Hyperfine Interactions* 225 (1-3) (2013) 137–141.

- 474 [15] M. Igarashi, J. Tostevin, Computer Program TWOFNR (Surrey University  
475 version), private communication.
- 476 [16] V. Modamio, et al., First Prototype of the NEDA detector array, INFN-  
477 LNL Annual Report (241).
- 478 [17] P.-A. Söderström, J. Nyberg, R. Wolters, Digital pulse-shape discrimina-  
479 tion of fast neutrons and rays, Nuclear Instruments and Methods in Physics  
480 Research Section A: Accelerators, Spectrometers, Detectors and Associated  
481 Equipment 594 (1) (2008) 79–89.
- 482 [18] G. Jaworski, et al.
- 483 [19] G. De France, EXOGAM: A  $\gamma$ -ray spectrometer for exotic beams, in: Ex-  
484 otic nuclei and atomic masses (ENAM 98). AIP Conference Proceedings,  
485 GANIL, BP 5027, 14076 Coen Cedex 5, France, 1998, pp. 977–980.
- 486 [20] S. L. Shepherd, P. J. Nolan, D. M. Cullen, D. Appelbe, J. Simpson, J. Gerl,  
487 M. Kaspar, A. Kleinboehl, I. Peter, M. Rejmund, H. Schaffner, C. Schlegel,  
488 G. De France, Measurements on a prototype segmented Clover detector,  
489 Nuclear Instruments and Methods in Physics Research Section A 434 (2)  
490 (1999) 373–386.
- 491 [21] J. Valiente-Dobón, et al., Status of the Gamma-Ray Spectrometer  
492 GALILEO, INFN-LNL Annual Report (95).
- 493 [22] M. Bellato, D. Bortolato, J. Chavas, R. Isocrate, G. Rampazzo, A. Triossi,  
494 D. Bazzacco, D. Mengoni, F. Recchia, Sub-nanosecond clock synchroniza-  
495 tion and trigger management in the nuclear physics experiment AGATA,  
496 Journal Of Instrumentation 8 (07) (2013) P07003–P07003.
- 497 [23] J.-N. Scheurer, M. Aiche, M. M. Aléonard, G. Barreau, F. Bourguine,  
498 D. Boivin, D. Cabaussel, J. F. Chemin, T. P. Doan, J. P. Goudour,  
499 M. Harston, A. Brondi, G. La Rana, R. Moro, E. Vardaci, D. Curien,  
500 Improvements in the in-beam  $\gamma$ -ray spectroscopy provided by an ancillary  
501 detector coupled to a Ge  $\gamma$ -spectrometer: the DIAMANT-EUROGAM II  
502 example, Nuclear Instruments and Methods in Physics Research Section A:  
503 Accelerators, Spectrometers, Detectors and Associated Equipment 385 (3)  
504 (1997) 501–510.
- 505 [24] E. Ronchi, P.-A. Söderström, J. Nyberg, E. A. Sundén, S. Conroy, G. Eric-  
506 son, C. Hellesen, M. G. Johnson, M. Weiszflog, An artificial neural network  
507 based neutron–gamma discrimination and pile-up rejection framework for  
508 the BC-501 liquid scintillation detector, Nuclear Instruments and Methods  
509 in Physics Research Section A: Accelerators, Spectrometers, Detectors and  
510 Associated Equipment 610 (2) (2009) 534–539.
- 511 [25] P.-A. Söderström, et al., Neutron detection and  $\gamma$ -ray rejection using ar-  
512 tificial neural networks with the liquid scintillators BC-501A and BC-537,  
513 Nuclear Instruments and Methods in Physics Research Section A: Acceler-  
514 ators, Spectrometers, Detectors and Associated Equipment to be submitted.